

AD-A127 787

ELECTRON ENERGY LOSS SPECTROSCOPY OF GALLIUM ARSENIDE
AND OTHER MATERIALS(U) MASSACHUSETTS INST OF TECH
CAMBRIDGE DEPT OF PHYSICS M H WEILER JUN 82

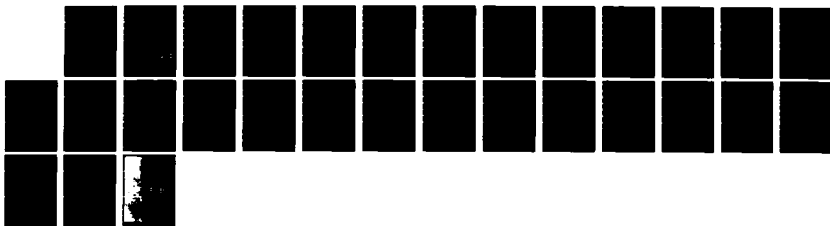
1/1

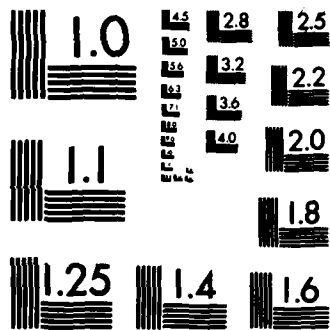
UNCLASSIFIED

AFOSR-TR-83-0370 F49620-79-C-0176

F/G 7/4

NL





MICROCOPY RESOLUTION TEST CHART
NATIONAL BUREAU OF STANDARDS-1963-A

UNCLASSIFIED

SECURITY CLASSIFICATION OF THIS PAGE (When Data Entered)

(11)

REPORT DOCUMENTATION PAGE		READ INSTRUCTIONS BEFORE COMPLETING FORM
1. REPORT NUMBER AFOSR-TR-83-0370	2. GOVT ACCESSION NO. AD-A127787	3. RECIPIENT'S CATALOG NUMBER
4. TITLE (and Subtitle) ELECTRON ENERGY LOSS SPECTROSCOPY OF GALLIUM ARSENIDE AND OTHER MATERIALS		5. TYPE OF REPORT & PERIOD COVERED FINAL REPORT .01 JUL 1979 - 30 JUN 1982
7. AUTHOR(s) Margaret H. Weiler		6. PERFORMING ORG. REPORT NUMBER
9. PERFORMING ORGANIZATION NAME AND ADDRESS Massachusetts Institute of Technology Department of Physics Cambridge, MA 02139		8. CONTRACT OR GRANT NUMBER(s) F49620-79-C-0176
11. CONTROLLING OFFICE NAME AND ADDRESS Air Force Office of Scientific Research / NE Building # 410 Bolling AFB, Washington, DC 20332		10. PROGRAM ELEMENT, PROJECT, TASK AREA & WORK UNIT NUMBERS 2306/B2 61102F
14. MONITORING AGENCY NAME & ADDRESS (if different from Controlling Office)		12. REPORT DATE June 1982
		13. NUMBER OF PAGES 09
		15. SECURITY CLASS. (of this report) UNCLASSIFIED
		15a. DECLASSIFICATION/DOWNGRADING SCHEDULE
16. DISTRIBUTION STATEMENT (of this Report) Approved for public release; distribution unlimited.		
17. DISTRIBUTION STATEMENT (of the abstract entered in Block 20, if different from Report)		
18. SUPPLEMENTARY NOTES		
19. KEY WORDS (Continue on reverse side if necessary and identify by block number)		
20. ABSTRACT (Continue on reverse side if necessary and identify by block number) The one-electron band theory of the electronic properties of solids the comparison between and experiment has been inhibited by the lack of experimental information relating specific features of the electronic band structure to their locations in the Brillouin zone. This information is necessary to understand such phenomena as hot-electron behavior and charge density waves. Present models for these phenomena postulate specific energy-band features at specific Brillouin zone locations; such locations have not been verified directly. Three years ago we began building an apparatus to use the technique of high-energy electron energy		

AD A 127787

DTIC FILE COPY

DTIC ELECTE
MAY 9 1983
S A D

loss spectroscopy (HELS) to provide the information on Brillouin zone location by allowing the observation of non-vertical transitions, that is, transitions between occupied and empty electron states with k-vector differing by as much as or more than a reciprocal lattice vector. The HELS data will allow us to map out the structure of both the conduction and valence bands through the Brillouin zone. Other techniques, such as photoemission, in general provide information only on the occupied (valence) bands. The HELS and angle-resolved photoemission (ARPES) techniques are complementary in that both measurements are needed to map out a complete band structure. HELS data on the dispersion of K-dependence of transitions between critical points (band maxima and minima) will provide information on the band curvatures or effective masses. We have constructed a HELS apparatus with a unique combination of high beam energy, high energy and momentum resolution with substantial beam current, and sophisticated data-taking techniques. Another unique feature of the apparatus is a double-selector monochromator with optimized coupling lens, which will enable us to study low-lying transitions at high resolution. The group has not only excellent experimental capability, but also the ability to carry out extensive analysis and interpretation of the data. Facilities and expertise available in the Center for Materials Science and Engineering at M.I.T. have enabled us to solve the substantial problem of preparing suitably thin samples.

UNCLASSIFIED

AFOSR-TR- 83 - 0370

FINAL SCIENTIFIC REPORT

July 1, 1979 - June 30, 1982

on

ELECTRON ENERGY LOSS SPECTROSCOPY
OF GALLIUM ARSENIDE AND OTHER MATERIALS

Submitted to

AIR FORCE OFFICE OF SCIENTIFIC RESEARCH

by

Department of Physics
Massachusetts Institute of Technology
Cambridge, Massachusetts 02139

Principal Investigator: Margaret H. Weiler
Assistant Professor
Department of Physics
Room 13-2145

Tel: (617) 253-4822

Accession For	
DTIC GRA&I	<input checked="" type="checkbox"/>
DTIC TAB	<input type="checkbox"/>
Unannounced	<input type="checkbox"/>
Justification	
Distribution/	
Availability Codes	
Dist	Special
A	



Approved for public release;
distribution unlimited.

83 05 06-149

TABLE OF CONTENTS

	Page No.
I. Introduction	2.
II. High-Energy Electron Energy Loss Spectroscopy (HELs) . .	4.
III. HELs Apparatus	6.
IV. Conclusion	12.

AIR FORCE OFFICE OF SCIENTIFIC RESEARCH (AFSC)
NOTICE OF CONFIDENTIALITY TO DTIC
This technical report is classified "Confidential" and is
approved for release to DTIC under E.O. 11652-1 and is
distributed under the terms of AFM 11-100-12.
MATTHEW J. HANSEN
Chief, Technical Information Division

I. INTRODUCTION

The one-electron band theory of the electronic properties of solids has been essential to the understanding of a wide variety of behavior of many materials, for example, the electrical and thermal properties of metals and semiconductors. The success of this model in describing these phenomena has made it a subject of intense study, both in the many calculational techniques such as OPW, APW, and LCAO, and in experimental tests such as electroreflectance, electron transport, magneto-optics, and photoemission. The comparison between theory and experiment has been inhibited by the lack of experimental information relating specific features of the electronic band structure to their locations in the Brillouin zone. This information is necessary to understand such phenomena as hot-electron behavior and charge density waves. Present models for these phenomena postulate specific energy-band features at specific Brillouin zone locations; such locations have not been verified directly.

Three years ago we began building an apparatus to use the technique of high-energy electron energy loss spectroscopy (HELs) to provide the information on Brillouin zone location by allowing the observation of non-vertical transitions, that is, transitions between occupied and empty electron states with \vec{k} -vectors differing by as much as or more than a reciprocal lattice vector. The HELs data will allow us to map out the structure of both the conduction and valence bands through the Brillouin zone. Other techniques, such as photoemission, in general provide information only on the occupied (valence) bands. The HELs and angle-resolved photoemission (ARPES) techniques are complementary in that both measurements are needed to map out a complete band structure. HELs data on the dispersion of \vec{k} -dependence of transitions between critical points (band maxima and minima) will provide information on the band curvatures or effective masses.

We have constructed a HELS apparatus with a unique combination of high beam energy, high energy and momentum resolution with substantial beam current, and sophisticated data-taking techniques. Another unique feature of the apparatus is a double-selector monochromater with optimized coupling lens, which will enable us to study low-lying transitions at high resolution. The group has not only excellent experimental capability, but also the ability to carry out extensive analysis and interpretation of the data. Facilities and expertise available in the Center for Materials Science and Engineering at M.I.T. have enabled us to solve the substantial problem of preparing suitably thin samples.

II. HIGH-ENERGY ELECTRON ENERGY LOSS SPECTROSCOPY (HELS)

The principle of high-energy electron energy loss spectroscopy is illustrated in Fig. 1a. The incident electron beam, with energy E_0 and momentum \vec{k} , is transmitted through a thin sample. The energy E_1 of the scattered electrons is measured as a function of their momentum \vec{k}' or of scattering angle. Structure in the scattered intensity is related to excitations of the sample at the loss energy $E = E_0 - E_1$ and wavevector $q = \vec{k} - \vec{k}'$. For electron energies of the order of 200 to 300 keV (required to penetrate the sample) and small scattering angles of the order of 0.25 degree, one can observe momentum transfers of the order of 1 \AA^{-1} which span the Brillouin zone.

The rate R for the scattering in Fig. 1a is given by

$$R(E, \vec{q}) = (4\pi e^2/q^2)^2 S(\vec{q}, E) \quad , \quad (1)$$

where $S(\vec{q}, E)$ is the structure factor given by

$$S(\vec{q}, E) = \sum_{i,f} |\langle f | (\sum_j e^{i\vec{q} \cdot \vec{r}_j}) | i \rangle|^2 \delta(E_f - E_i - E) \quad . \quad (2)$$

For small q , in the random phase approximation, this can be written⁸

$$S(\vec{q}, E) = -(q^2/4\pi e^2) \text{Im} [1/\epsilon(\vec{q}, E)] \quad (3)$$

where $\epsilon(\vec{q}, E)$ is the dielectric constant.

Figure 1b illustrates a typical transition observable using electron energy loss spectroscopy. Suppose the energy of the upper valence band near the point ($k = 0$) can be written

$$E_V(\vec{k}) = -\hbar^2 k^2 / 2m_V \quad , \quad (4)$$

where m_V is the hole effective mass, and the energy of the conduction band minimum at \vec{k}_0 is given by

$$E_{\vec{k}_0}^{\vec{k}} = E_g' + \hbar^2(k_{\parallel} - k_0)^2/2m_{\parallel} + \hbar^2 k_{\perp}^2/2m_{\perp} \quad , \quad (5)$$

where m_{\parallel} and m_{\perp} are, respectively, the longitudinal and transverse effective masses, and k_{\parallel} and \vec{k}_{\perp} are the components of \vec{k} parallel and perpendicular to \vec{k}_0 . The transition rate R is approximately proportional to joint density of states function

$$D(\vec{q}, E) = \frac{\mu_{\parallel}^{1/2} \mu_{\perp}}{(2\hbar^2)^{3/2}} [E - E_g' - \hbar^2(q_{\parallel} - k_0)^2/2m_{\parallel}' - \hbar^2 q_{\perp}^2/2m_{\perp}']^{1/2} \quad , \quad (6)$$

where μ_{\parallel} and μ_{\perp} are the reduced effective masses $\mu_{\parallel}^{-1} \equiv m_{\parallel}^{-1} + m_V^{-1}$ and $\mu_{\perp}^{-1} \equiv m_{\perp}^{-1} + m_V^{-1}$, and $m_{\parallel, \perp}' \equiv m_{\parallel, \perp} + m_V$. This transition rate has an edge, and the derivative spectrum a peak, at the zero of the square brackets in Eq. (6). By observing the peak E at values of q_{\parallel} and q_{\perp} near \vec{k}_0 , we can measure the energy E_g' of the conduction band minimum, the location \vec{k}_0 in the Brillouin zone, and the effective masses m_{\parallel} and m_{\perp} based on the known valence band effective mass m_V . For a material where the valence band is not known, these transitions will provide valuable evidence for mapping out the band structure in combination with data from other experiments, such as photoemission.

For a momentum transfer \vec{q} which does not correspond to a transition between a valence band critical point and a conduction band critical point, the transition rate R will still exhibit peaks at new joint critical points, where a conduction band at $\vec{k} + \vec{q}$ is parallel to a valence band at \vec{k} . While these transitions will be weaker than those in Eq. (6), we expect them to provide valuable additional data for band-structure determination.

III. HELS APPARATUS

We have designed and constructed an apparatus to carry out HELS studies using the inelastic scattering of 230-300 keV electrons, measuring energy loss up to 1000 eV with resolutions from 0.03 to 0.1 eV and momentum transfer up to 7 \AA^{-1} with resolutions from 0.02 to 0.2 \AA^{-1} . The apparatus is illustrated schematically in Fig. 2. It consists of an electron monochromator, in the vacuum chamber on the left, accelerator tubes, deflection coils, sample chamber, decelerator tubes, and an analyzer in the right vacuum chamber, with three ion pumps to maintain the pressure in each chamber in the low 10^{-9} Torr range.

The monochromator is a unique double-selector system designed by us. It is shown schematically in Figure 3. It consists of two hemispherical energy selectors. The first selector acts as a pre-selector, passing a beam of a larger energy spread ΔE_1 than the spread ΔE_2 of the second selector. One advantage of this double selector system is that the output beam current is larger, for a given ΔE_2 , than for a single selector of input energy width $\Delta E_0 > \Delta E_1$. The reason is that the input beam for each monochromator is operated in the space-charge limited condition; the pre-selected beam has a larger fraction of the electrons within the final width ΔE_2 , so that the output current can be larger for this case. A second advantage of the double selector system is the same advantage as in optical systems: one finds a significant reduction in the wings of the output line shape, because signals due to internal scattering of the beam are eliminated. In the case of an electron beam, our design has completely eliminated the "ghost" lines which occur in standard systems due to electrons of the wrong energy which pass through the output slits after one or more reflections from the surfaces of the hemispheres. In each of our energy selectors, all of the electrons within the

input energy width are confined to paths far away from the surfaces and cannot be reflected from them.

The difficulty with the double monochromator system, and the reason that an optimum system has not been used before, is the problem of finding an electron lens system which couples the two selectors over a range of operating conditions. Brunt, et al.¹ used a double monochromator system consisting of two identical selectors with no coupling lens at all. We have been able to design the necessary coupling lens system using our own computer program which rapidly computes and displays graphically the extremes of the electron beam propagating through a given lens system with given input properties.

In our design we relied on the results of Kuyatt and Simpson,² who have made extensive calculations and measurements on hemispherical energy selectors. Using their results for the optimum pass energy E , angular half-width α , and slit width w , for a given energy resolution ΔE , we designed two selectors, coupled by a lens system, with near-optimum parameters for energy resolutions from 0.02 to 0.10eV. These parameters are listed in Table I, where the parameters β_1 , β_2 , and r represent deviation from the optimum conditions in the equations

$$\begin{aligned} E_1 &= 116\Delta E_0\Delta E_1 R_1^2 \beta_1 / r^2 & E_2 &= 116\Delta E_1\Delta E_2 R_2^2 \beta_2 \\ \alpha_1 &= r\sqrt{\Delta E_1/2E_1} & \alpha_2 &= \sqrt{\Delta E_2/2E_2} \\ w_1 &= 2R_1\Delta E_1/E_1 & w_2 &= 2R_2\Delta E_2/E_2 \end{aligned} \quad (7)$$

We chose the optimum performance $\beta_1 = \beta_2 = r = 1$ at an energy resolution $\Delta E_z = 0.02\%$. At this resolution the calculated output current of 0.094 μ A is a factor 1.9 larger than the current from a single optimized selector with the same resolution. The mean hemisphere radii R_1 and R_2 were chosen so that the monochromator would fit into the largest standard 8" O.D. vacuum chamber. The

Table I. Calculated operating parameters for double monochromator system with $R_1 = 3.175\text{cm} = 1.25''$ and $R_2 = 4.445\text{cm} = 1.75''$.

ΔE_2	0.02	0.05	0.10	eV
β_1	0.360	0.595	0.855	
r	0.750	0.965	1.156	
β_2	1	0.662	0.475	
ΔE_1	0.077	0.117	0.163	eV
E_1	14.46	21.83	30.40	eV
α_1	0.039	0.050	0.060	rad
w_1	0.034	0.034	0.034	cm
E_2	3.55	8.87	17.73	eV
α_2	0.053	0.053	0.053	rad
w_2	0.050	0.050	0.050	cm
I_1^{in}	3.19	9.79	23.09	μA
$I_1^{out} = I_2^{in}$	0.727	2.88	8.13	μA
I_2^{out}	0.094	0.740	3.61	μA

design of the coupling lens is shown in Figs. 4, 5 and 6, which give the computer-calculated beam parameters for the three energy resolutions given in Table I.

The analyzer consists of a single hemispherical selector with an input lens identical to the monochromator output lens in Fig. 3, and a simple output lens terminating at an electron multiplier. Since space charge effects are negligible a double-selector analyzer offers no advantage in beam current and also does not eliminate reflections.

The monochromator output lens, and analyzer input lens, contain a zoom lens designed following the suggestion of Dr. J. Ritsko of Xerox. The design, as shown in Fig. 3 and in the computer plots in Figs. 7 and 8, consists of a series of gaps of different diameter, with the voltage step applied at only one "active" gap. It provides six steps of variable magnification, with fixed object and image position, to give momentum resolutions from 0.02 to 0.20 \AA^{-1} .

After leaving the monochromator the beam enters the accelerator tubes (see Fig. 2), the electron-optical properties of which were calculated by the method of relaxation and by relativistic ray-tracing. The beam then enters the sample chamber inside a large high-voltage terminal with large-radius corners to prevent air-breakdown to the surrounding grounded cage. Just before entering the sample chamber the beam is deflected by two high-resolution coils to introduce the scattering angle for the desired momentum transfer. The sample is held on a sample manipulator. The electrons leaving the sample at small angles pass through the decelerator tubes into the analyzer. The entire system is shielded to limit magnetic fields to $\sim 0.005 \text{ G}$.

Provision is made for controlling the sample temperature using a closed-cycle refrigerator which will enable us to set the temperature from about 20 to 350K. The He compressor is outside the grounded cage; plastic hoses connect the

compressor to the refrigerator in the terminal, which receives control signals over the IEEE-488 bus-optical fiber link.

The vacuum system is divided into three chambers by gate valves near the sample chamber, so that vacuum can be maintained in the monochromator, analyzer, and accelerator and decelerator tubes, while samples are changed. The system has gradually become cleaner and cleaner, so that a pressure of 2×10^{-9} mb is measured in the monochromator chamber after only a few days' pumping, without baking.

The other major part of the HELS apparatus consists of the various electronics components. A diagram is given in Fig. 9. The electronics systems consist of power supplies for the monochromator and analyzer lens and deflector voltages, an energy loss power supply, a DEC MINC-11 computer, a high-voltage power supply and isolation transformer for the terminal, electronics to control the deflection coils and stepping motors with two optical-fibers systems to receive signals from the computer, and systems for collecting signals from the electron multiplier.

Our experiment consists of measuring the intensity of scattered electrons as a function of energy loss ΔE . We vary this energy by controlling a programmable power supply which raises the reference or ground voltage in the analyzer with respect to the cathode ground. By varying ΔE , scattered electrons with different kinetic energy are passed by the analyzer energy selector. The present power supply along with an operational amplifier gives a range of ΔE of about 1keV.

The scattered electron intensity is measured by counting pulses from the electron multiplier positioned after the output slit of the analyzer. The pulses are formed by an amplifier/discriminator. For the case of high beam intensity where the pulses are too rapid to count individually, we have a frequency counter, and for even higher rates, a current-measuring systems.

A number of programs have been written to control the stepping motors and deflection coils and to collect and reduce our data. One program steps the energy-loss voltage, collects a fixed number counts from the electron multiplier, and records the time interval at each step. A second program collects the data for multiple scattering by estimating the energy-loss intensity I_2 due to double-scattering events and subtracting this from the data using the convolution

$$I_2(\Delta E) = \frac{1}{2} \int_0^{\Delta E} I(\Delta E') P_1(\Delta E - \Delta E') dE' , \quad (8)$$

where the single scattering probability per energy interval is $P_1 \approx I(\Delta E)/I_0 \Delta E_r$, with I_0 the incident beam intensity and ΔE_r the energy resolution. Another set of programs is being written, to carry out a Kramers-Kronig analysis of the data to obtain the real and imaginary parts of the dielectric function.

With this apparatus we have now produced a beam of about 10 nA stable and well focussed on a phosphor screen at the center of the sample chamber with an estimated resolution of 0.05 eV. This compares favorably with the 6nA beam used by Dr. J. Rotsko of Xerox, at 0.07eV resolution. We are in the process of directing our beam through the analyzer to the electron multiplier. For the purpose of detecting current at the analyzer lens elements we modulate the beam intensity at 80 Hz. We accelerate the electrons routinely to 220 keV and have gone up to 240 keV; the accelerator and decelerator tubes should gradually become conditioned, enabling us eventually to use the full 300 kV provided by the power supply.

During the past year, with additional support from Sloan funds at M.I.T., we significantly improved the stability of our beam by replacing the battery power supplies for the deflector elements by regulated supplies using Zener diodes. With this improved stability we now have brought the beam through the analyzer

lens systems, through the series of apertures and onto the energy-selecting hemispheres. We are optimizing the beam, preparing to collect the electrons on the electron multiplier.

A major requirement of the HELS experiment is to have samples thin enough to transmit the electron beam without significant multiple scattering. Our task of sample preparation is made much easier by the facilities and expertise available in the Center for Materials Science and Engineering, particularly the facilities of the electron microscopy group (Prof. John Vander Sande) and those of Prof. Harry Gatos in the Materials Science Department. We have explored and are continuing to explore a number of techniques, such as ion milling, various methods of etching masked samples, and sputtering on dissolvable or electron-transparent substrates. Using selective etching we have obtained for samples of GaAs, 0.1 and 0.2 μ m thick, by removing from them from GaAs/AlGaAs/GaAs structures kindly prepared for us by Dr. R. Logan of Bell Laboratories.

IV. CONCLUSION

As is evident from the above description, we have designed and constructed a large and complex apparatus which has unique capabilities to determine the electronic states in materials. We encountered many delays along the way, in finding good people, in obtaining ordered items of equipment, repairing defective items, and in solving a number of problems such as learning how to prevent arcing among the monochromator and analyzer lens elements. We have solved all these problems and are confident that the apparatus will work as designed very soon. We are encouraged by the attainment of a beam with good current, using lens voltages close to those of the original design, that we will encounter no more major problems in getting the beam through the analyzer and beginning our experiments.

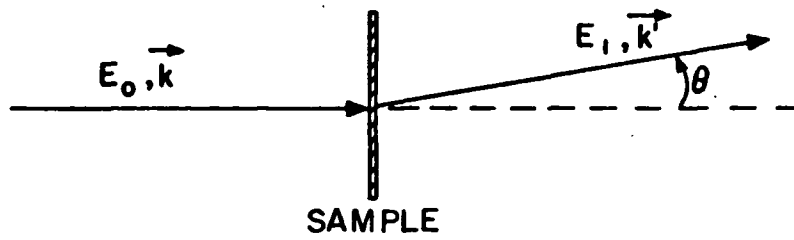
References

1. J. N. H. Brunt, F. H. Read, and G. C. King, J. Phys. E 10, 101 (1977).
2. C. E. Kuyatt and J. Simpson, Rev. Sci. Instrum. 38, 103 (1967).

FIGURE CAPTIONS

- Fig. 1. a) Diagram of electron scattering. b) Illustration of a non-vertical transition.
- Fig. 2. Schematic diagram of the HELS apparatus.
- Fig. 3. Schematic diagram of the double-selector monochromator assembly.
- Fig. 4. Computer output for the monochromator coupling lens for $\Delta E_2 = 0.020\text{eV}$. All lengths are given in inches. Windows are marked by vertical dashed lines, pupils by vertical dot-dashed lines. The input pupil is at infinity. The initial window is at the output of selector #1; the final window is at input of selector #2. An aperture (slit) is placed at the output window of lens #2.
- Fig. 5. Computer output for the monochromator coupling lens for $\Delta E_2 = 0.05\text{eV}$.
- Fig. 6. Computer output for the monochromator coupling lens for $\Delta E_2 = 0.10\text{eV}$.
- Fig. 7. Computer output for the zoom lens, for momentum resolution $\Delta q = 0.2\text{\AA}^{-1}$. The input window is the output of the first half of the monochromator lens system. The zoom lens consists of a number of gaps, at one of which, here, the last, the step from 714 to 5000V is made. The output window is placed at the required location for the accelerator tube, with the pupil also at the required position.
- Fig. 8. Computer output for the zoom lens, for momentum resolution $\Delta q = 0.02\text{\AA}^{-1}$. Here the voltage step is at the first gap.
- Fig. 9. Electronics diagram for the HELS apparatus.

a)



b)

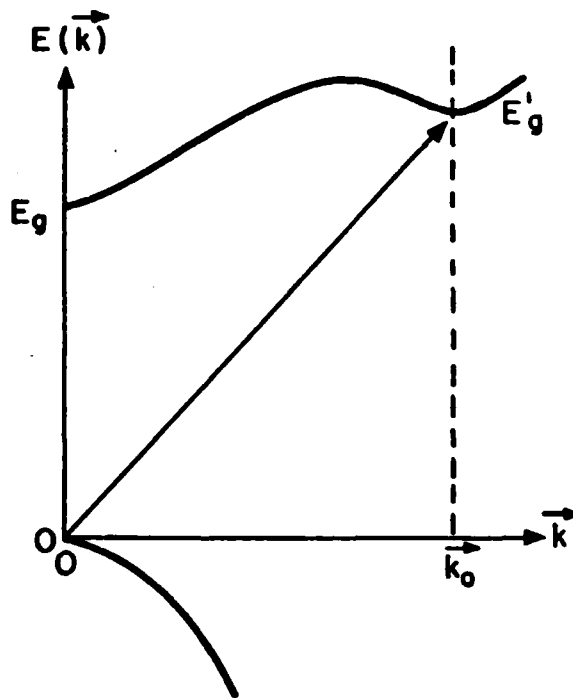


Fig. 1

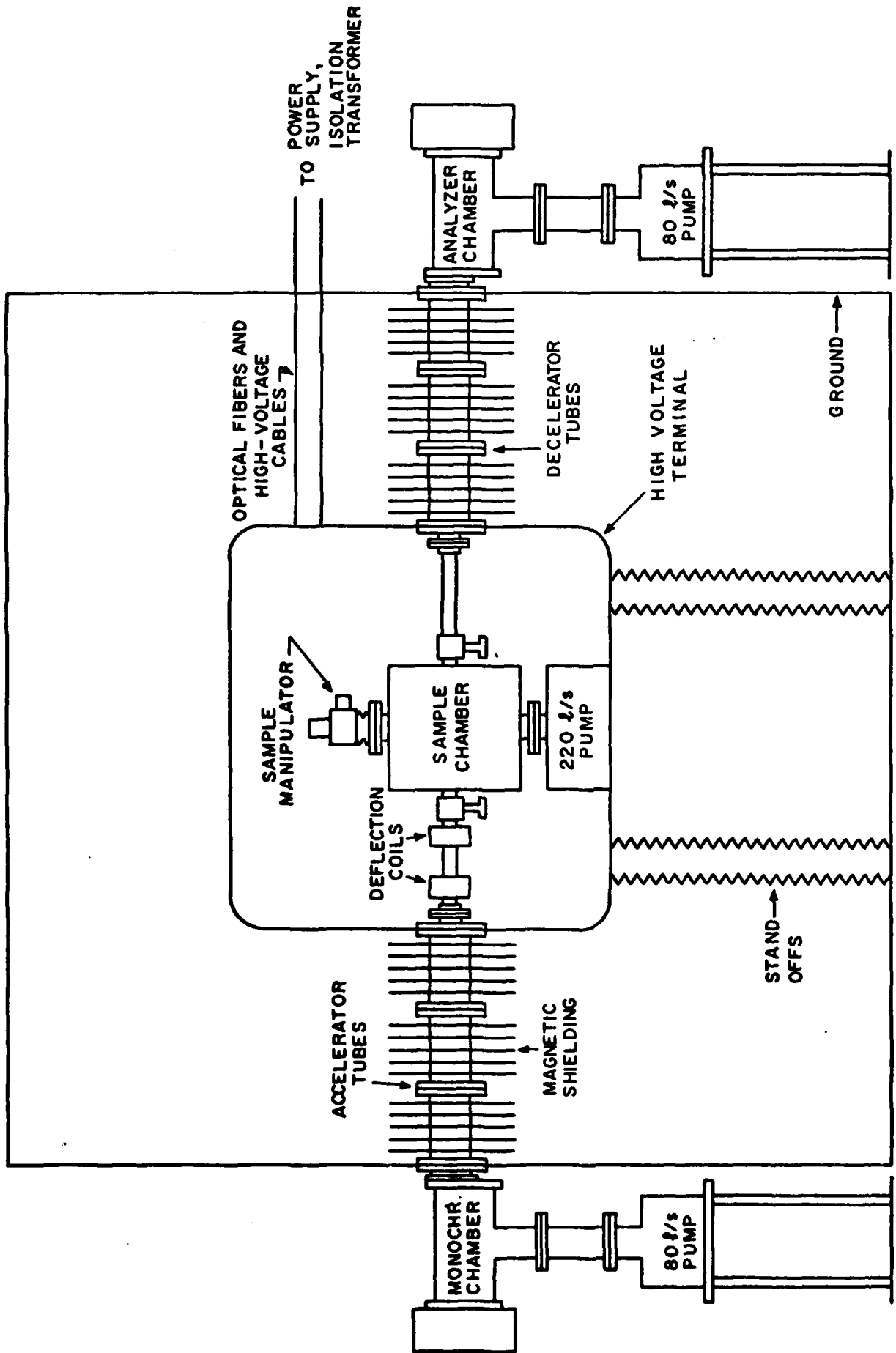


Fig. 2

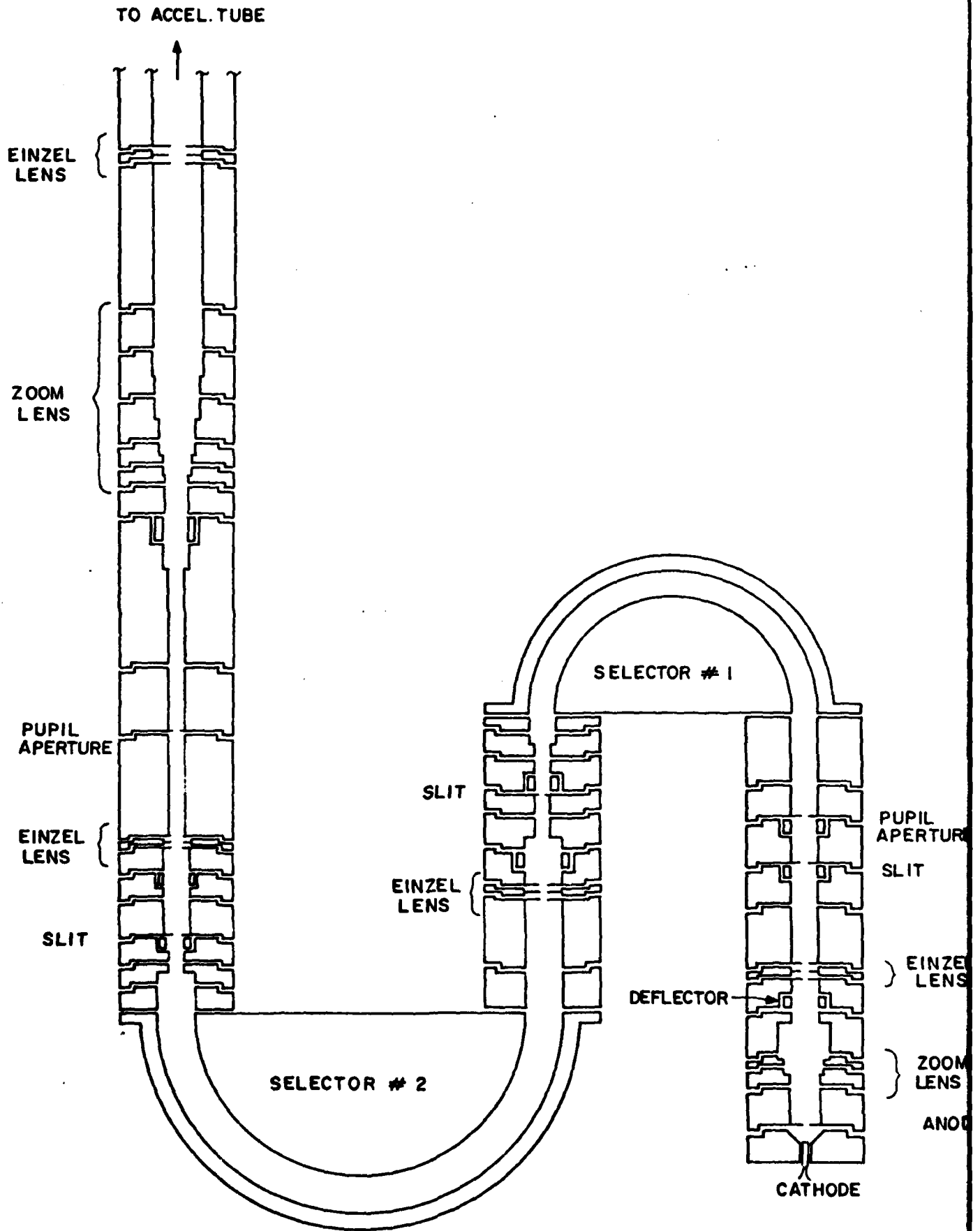


Fig. 3

SELECTOR COUPLING LENS, $\Delta E_2 = 0.02\text{eV}$

WINDOW DIAMETER= .0134

ENTRANCE POSITION= 0

INPUT PENCIL ANGLE= .0388

LENS#	VOLT.	DIAMETER	LENS POSIT	WIN POSIT	WIN DIAM	PUP POSIT	PUP DIAM
0	14.460						
1	503.000	.250	.180	-1.964E-01	+1.324E-02	+2.723E-01	+6.216E-03
2	43.160	.140	.397	+7.064E-01	+1.067E-02	-4.461E-01	+6.052E-03
3	491.600	.125	.563	+1.715E+00	+2.021E-02	+1.138E+00	+5.089E-03
4	69.000	.125	1.702	+1.699E+00	+1.992E-02	+2.496E+00	+7.139E-03
5	3.547	.375	2.481	+2.884E+00	+2.001E-02	+5.329E+01	+5.275E+00

EINZEL PARAMETER U= .386896833158 CENTER APERTURE VOLTAGE= 69

EINZEL INNER RADIUS= .05

OUTER RADIUS= .0375

BEAM SCALING FACTOR = 1

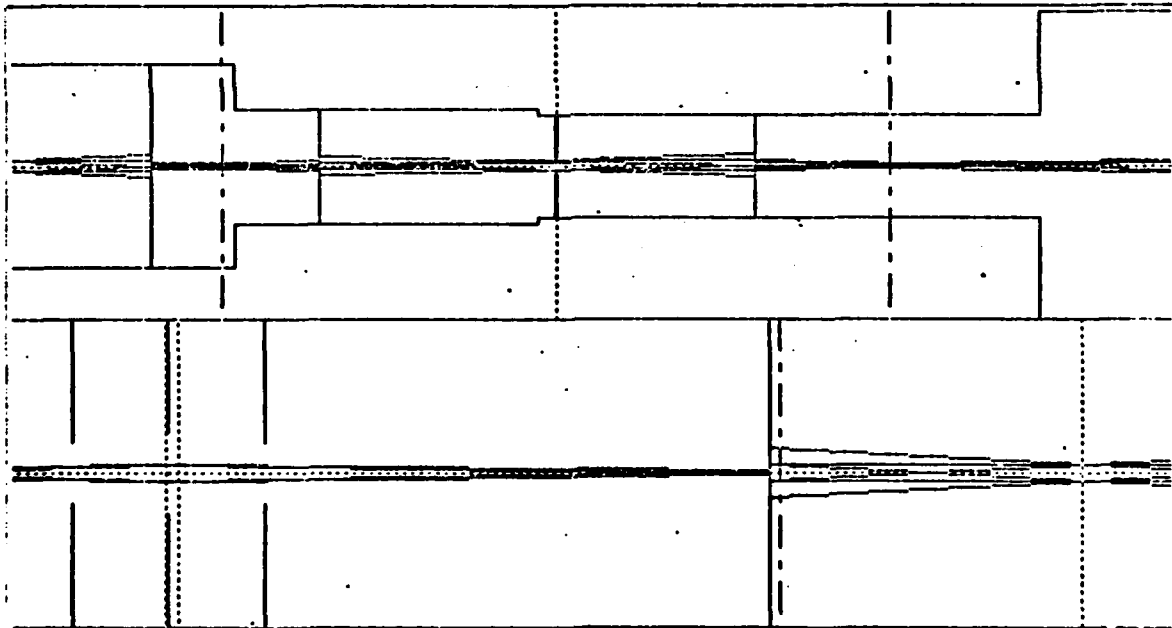


Fig. 4

SELECTOR COUPLING LENS, $\Delta E_2 = 0.05\text{eV}$

WINDOW DIAMETER= .0134 ENTRANCE POSITION= 0
INPUT PENCIL ANGLE= .04992

LENS#	VOLT.	DIAMETER	LENS POSIT	WIN POSIT	WIN DIAM	PUP POSIT	PUP DIAM
0	21.830						
1	1229.300	.250	.180	-2.454E-01	+1.347E-02	+2.313E-01	+6.307E-03
2	1229.300	.140	.397	+7.060E-01	+9.992E-03	+7.965E+01	+4.454E+00
3	1229.300	.126	.963	+1.711E+00	-1.880E-02	+1.111E+00	+5.686E-03
4	182.000	.125	1.702	+1.695E+00	+1.874E-02	+2.499E+00	+7.642E-03
5	8.870	.375	2.481	+2.884E+00	+1.875E-02	-3.850E+01	+4.622E+00

EINZEL PARAMETER U= .392802038371 CENTER APERTURE VOLTAGE= 192
EINZEL INNER RADIUS= .05 OUTER RADIUS= .0375
BEAM SCALING FACTOR = 1

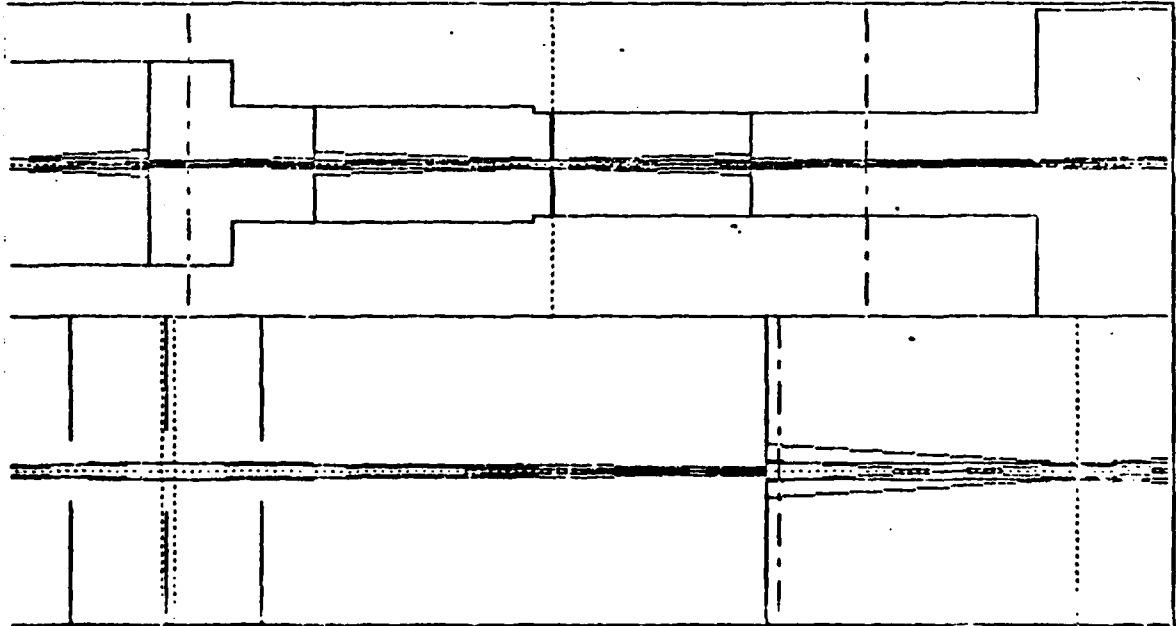


Fig. 5

SELECTOR COUPLING LENS, $\Delta E_2 = 0.10$ eV

WINDOW DIAMETER= .0134

ENTRANCE POSITION= 0

INPUT PENCIL ANGLE= .05962

LENS#	VOLT.	DIAMETER	LENS POSIT	MIN POSIT	MIN DIAM	PUP POSIT	PUP DIAM
0	30.400						
1	2396.000	.250	.180	-2.879E-01	+1.360E-02	+2.064E-01	+6.565E-03
2	245.730	.140	.397	+7.058E-01	+9.433E-03	+2.533E+00	+1.092E-01
3	2457.300	.126	.963	+1.709E+00	+1.769E-02	+1.094E+00	+6.204E-03
4	375.000	.125	1.702	+1.693E+00	+1.773E-02	+2.499E+00	+8.103E-03
5	17.730	.375	2.481	+2.884E+00	+1.770E-02	-3.852E+01	+4.901E+00

EINZEL PARAMETER U= .396294168845 CENTER APERTURE VOLTAGE= 375

EINZEL INNER RADIUS= .05 OUTER RADIUS= .0375

BEAM SCALING FACTOR = 1

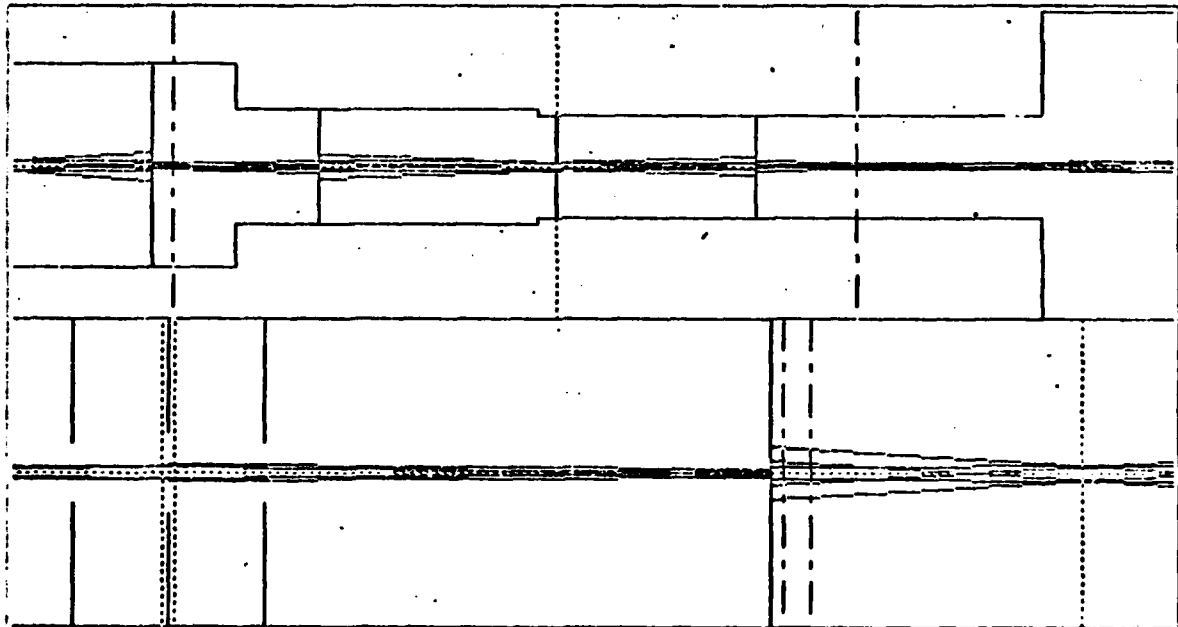


Fig. 6

ZOOM LENS, $\Delta q = 0.20\text{\AA}^{-1}$

WINDOW DIAMETER= .01

ENTRANCE POSITION= 0

INPUT PENCIL ANGLE= .0165

LENS#	VOLT.	DIAMETER	LENS POSIT	WIN POSIT	WIN DIAM	PUP POSIT	PUP DIAM
0	714.000						
1	714.000	.206	.472	+3.515E-07	+1.000E-02	+5.240E+05	+1.729E+04
2	714.000	.284	.691	-7.697E-07	+1.000E-02	+3.037E+05	+1.002E+04
3	714.000	.362	.950	-1.364E-06	+1.000E-02	+2.284E+05	+7.537E+03
4	714.000	.452	1.361	-6.148E-06	+1.000E-02	+1.905E+05	+6.298E+03
5	714.000	.500	1.804	-1.681E-05	+1.000E-02	+1.657E+05	+5.459E+03
6	5000.000	.495	2.230	+3.766E+00	+4.676E-03	+3.060E+00	+1.883E-02
7	420.000	.200	3.730	+3.731E+00	+4.478E-03	+4.923E+00	+3.319E-02

EINZEL PARAMETER U= .343390896122 CENTER APERTURE VOLTAGE= 420

EINZEL INNER RADIUS= .08 OUTER RADIUS= .06

BEAM SCALING FACTOR = 1

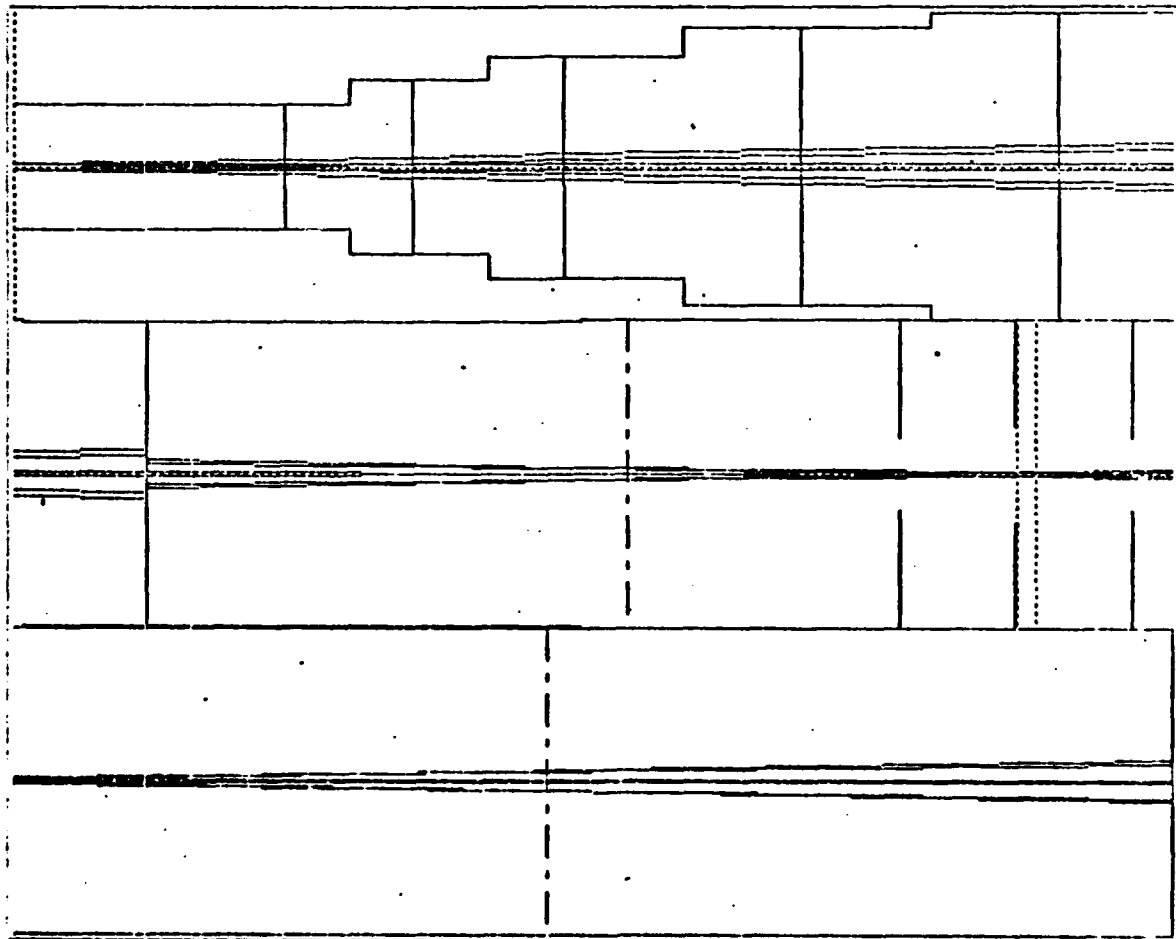


Fig. 7

ZOOM LENS, $\Delta q = 0.02\text{\AA}^{-1}$

WINDOW DIAMETER= .01

ENTRANCE POSITION= 0

INPUT PENCIL ANGLE= .0165

LENS#	VOLT.	DIAMETER	LENS POSIT	WIN POSIT	WIN DIAM	PUP POSIT	PUP DIAM
0	714.000						
1	5000.000	.206	.472	+3.698E+00	+4.586E-02	+8.175E-01	+7.836E-03
2	5000.000	.284	.691	+3.698E+00	+4.586E-02	+8.175E-01	+7.836E-03
3	5000.000	.362	.950	+3.698E+00	+4.586E-02	+8.175E-01	+7.836E-03
4	5000.000	.452	1.361	+3.698E+00	+4.586E-02	+8.175E-01	+7.836E-03
5	5000.000	.500	1.804	+3.698E+00	+4.586E-02	+8.175E-01	+7.836E-03
6	5000.000	.495	2.230	+3.698E+00	+4.586E-02	+8.175E-01	+7.836E-03
7	1300.000	.200	3.730	+3.683E+00	+4.808E-02	+4.884E+00	+3.116E-03

EINZEL PARAMETER U= .477816253181 CENTER APERTURE VOLTAGE= 1300

EINZEL INNER RADIUS= .08 OUTER RADIUS= .06

BEAM SCALING FACTOR = 1

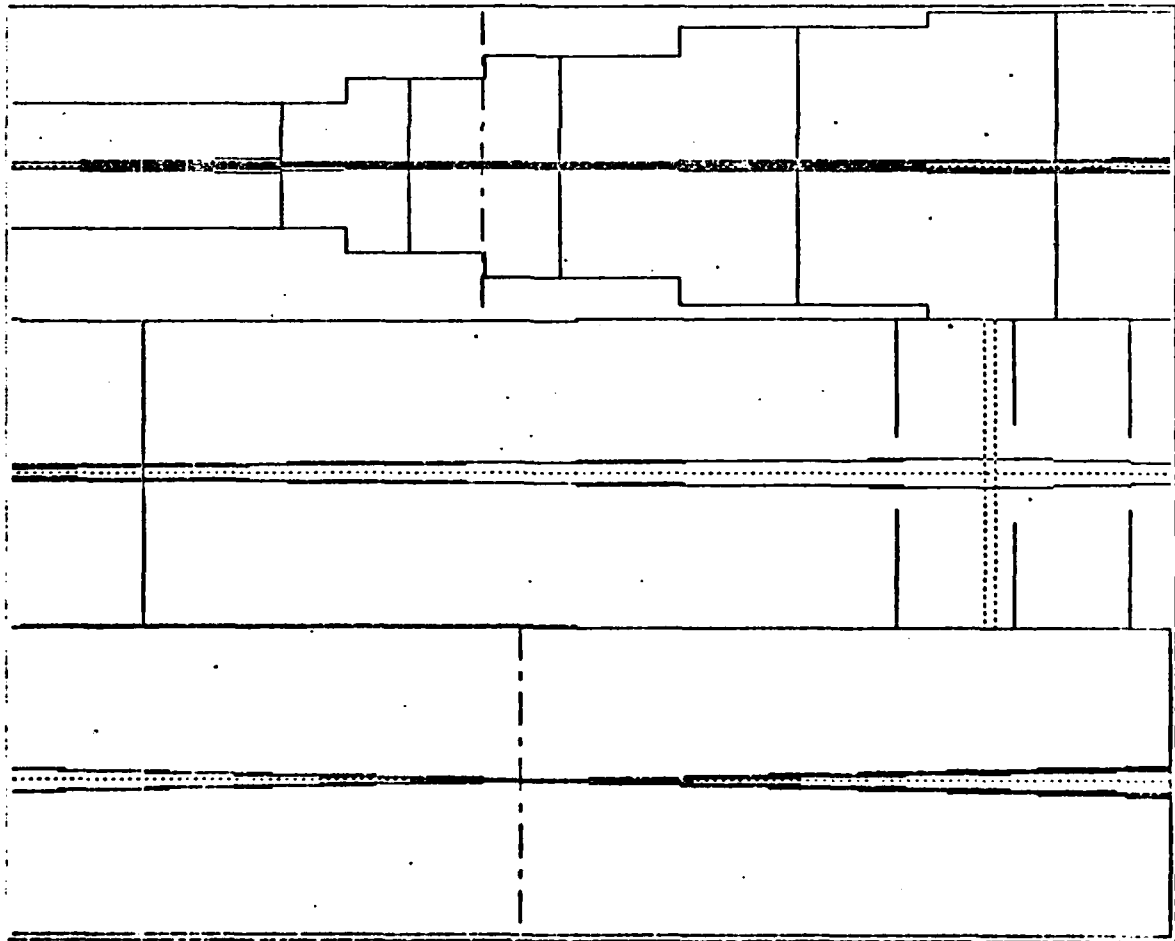


Fig. 8

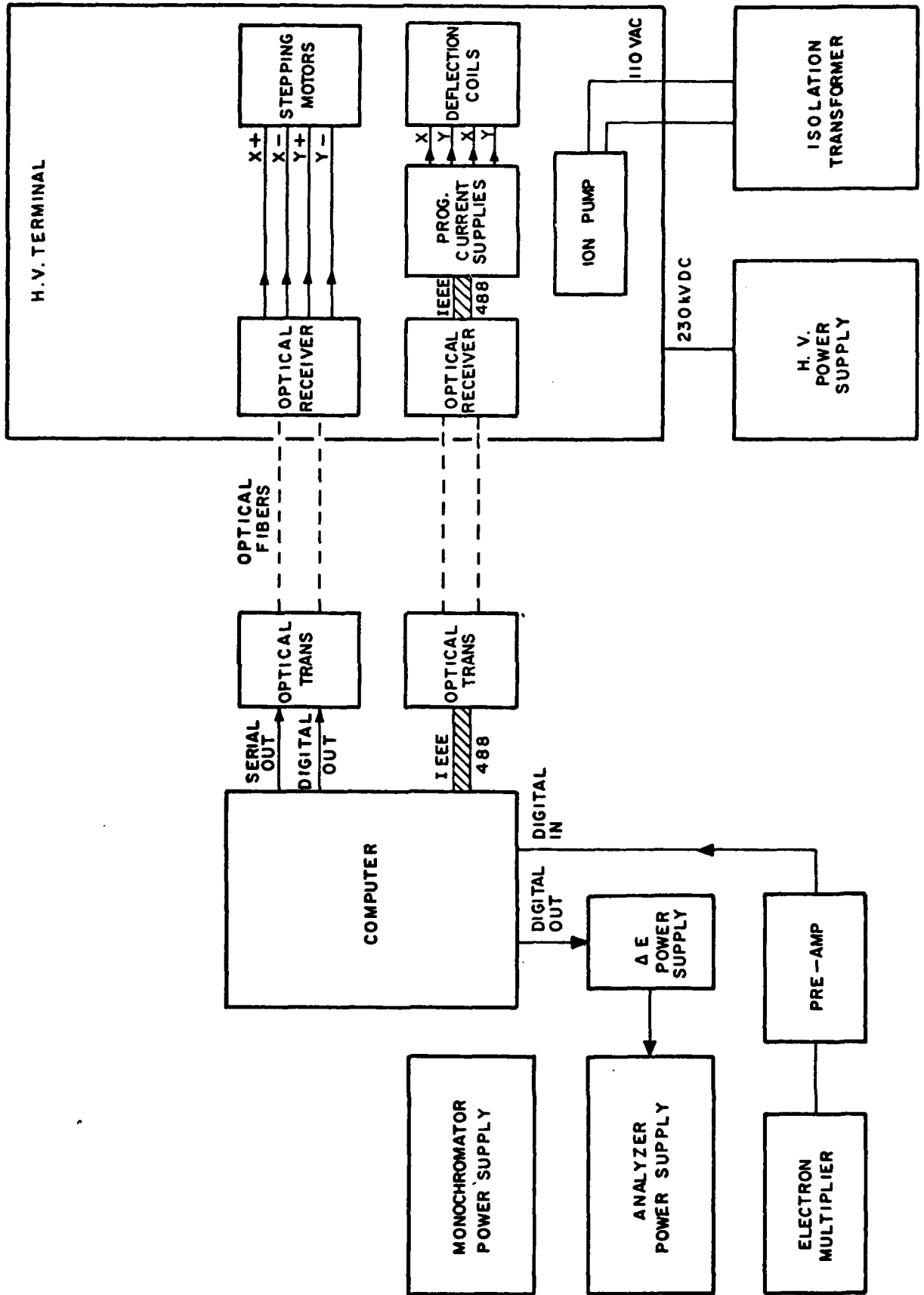


Fig. 9

UNCLASSIFIED

SECURITY CLASSIFICATION OF THIS PAGE (When Data Entered)

REPORT DOCUMENTATION PAGE		READ INSTRUCTIONS BEFORE COMPLETING FORM	
1. REPORT NUMBER AFOSR-TR- 83 - 03870	2. GPO ACCESSION NO.	3. RECIPIENT'S CATALOG NUMBER	
4. TITLE (and Subtitle) ELECTRON ENERGY LOSS SPECTROSCOPY OF GALLIUM ARSENIDE AND OTHER MATERIALS	5. TYPE OF REPORT & PERIOD COVERED FINAL REPORT 01 JUL 1979 - 30 JUN 1982		
	6. PERFORMING ORG. REPORT NUMBER		
7. AUTHOR(s) Margaret H. Weiler	8. CONTRACT OR GRANT NUMBER(s) F49620-79-C-0176		
9. PERFORMING ORGANIZATION NAME AND ADDRESS Massachusetts Institute of Technology Department of Physics Cambridge, MA 02139	10. PROGRAM ELEMENT, PROJECT, TASK AREA & WORK UNIT NUMBERS 2306/B2 61102F		
11. CONTROLLING OFFICE NAME AND ADDRESS Air Force Office of Scientific Research Building # 410 Bolling AFB, Washington, DC 20332	12. REPORT DATE JUNE 1982		
	13. NUMBER OF PAGES 09		
14. MONITORING AGENCY NAME & ADDRESS (if different from Controlling Office)	15. SECURITY CLASS. (of this report) UNCLASSIFIED		
	15a. DECLASSIFICATION/DOWNGRADING SCHEDULE		
16. DISTRIBUTION STATEMENT (of this Report) <p style="text-align: center;">Approved for public release; distribution unlimited.</p>			
17. DISTRIBUTION STATEMENT (of the abstract entered in Block 20, if different from Report)			
18. SUPPLEMENTARY NOTES			
19. KEY WORDS (Continue on reverse side if necessary and identify by block number)			
20. ABSTRACT (Continue on reverse side if necessary and identify by block number) The one-electron band theory of the electronic properties of solids the comparison between and experiment has been inhibited by the lack of experimental information relating specific features of the electronic band structure to their locations in the Brillouin zone. This information is necessary to understand such phenomena as hot-electron behavior and charge density waves. Present models for these phenomena postulate specific energy-band features at specific Brillouin zone locations; such locations have not been verified directly. Three years ago we began building an apparatus to use the technique of high-energy electron energy			

UNCLASSIFIED

UNCLASSIFIED

SECURITY CLASSIFICATION OF THIS PAGE(When Data Entered)

loss spectroscopy (HELS) to provide the information on Brillouin zone location by allowing the observation of non-vertical transitions; that is, transitions between occupied and empty electron states with k-vector differing by as much as or more than a reciprocal lattice vector. The HELS data will allow us to map out the structure of both the conduction and valence bands through the Brillouin zone. Other techniques, such as photoemission, in general provide information only on the occupied (valence) bands. The HELS and angle-resolved photoemission (ARPES) techniques are complementary in that both measurements are needed to map out a complete band structure. HELS data on the dispersion of K-dependence of transitions between critical points (band maxima and minima) will provide information on the band curvatures or effective masses. We have constructed a HELS apparatus with a unique combination of high beam energy, high energy and momentum resolution with substantial beam current, and sophisticated data-taking techniques. Another unique feature of the apparatus is a double-selector monochromator with optimized coupling lens, which will enable us to study low-lying transitions at high resolution. The group has not only excellent experimental capability, but also the ability to carry out extensive analysis and interpretation of the data. Facilities and expertise available in the Center for Materials Science and Engineering at M.I.T. have enabled us to solve the substantial problem of preparing suitably thin samples.

UNCLASSIFIED

SECURITY CLASSIFICATION OF THIS PAGE(When Data Entered)

END

FILMED

6-83

DTIC